

Review

Open Access

Multi-material multi-photon 3D laser micro- and nanoprinting

Liang Yang¹, Frederik Mayer^{1,2}, Uwe H. F. Bunz^{3,4}, Eva Blasco^{1,3,4} and Martin Wegener^{1,2*}

Abstract

Three-dimensional (3D) laser micro- and nanoprinting based upon multi-photon absorption has made its way from early scientific discovery to industrial manufacturing processes, e.g., for advanced microoptical components. However, so far, most realized 3D architectures are composed of only a single polymeric material. Here, we review 3D printing of multi-materials on the nano- and microscale. We start with material properties that have been realized, using multi-photon photoresists. Printed materials include bulk polymers, conductive polymers, metals, nanoporous polymers, silica glass, chalcogenide glasses, inorganic single crystals, natural polymers, stimuli-responsive materials, and polymer composites. Next, we review manual and automated processes achieving dissimilar material properties in a single 3D structure by sequentially photo-exposing multiple photoresists as 3D analogs of 2D multicolor printing. Instructive examples from biology, optics, mechanics, and electronics are discussed. An emerging approach – without counterpart in 2D graphical printing – prints 3D structures combining dissimilar material properties in one 3D structure *by using only a single photoresist*. A controlled stimulus applied during the 3D printing process defines and determines material properties on the voxel level. Change of laser power and/or wavelength, or application of quasi-static electric fields allow for the seamless manipulation of desired materials properties.

Introduction

Multiple materials in three-dimensional (3D) additive manufacturing, that is 3D printing, are analogous to colors in 2D graphical printing. A set of primary colors and “primary materials” are the base. The different primary colors or materials need to form inks, printable by a single instrument. Last, a small set of primary ingredients must create thousands of different colors (materials), without the need for physically/chemically mixing them within one 2D pixel or 3D voxel, respectively. In 2D graphical printing

this step is accomplished by dithering¹ or half-tone printing. By filling, e.g., 50% of a white paper with black pixels, the observer perceives a homogeneous gray area, if pixel size and the spacing between the pixels are sufficiently small, i.e., unresolved for the observer.

Today’s multi-material 3D material printing is less advanced than multi-color 2D graphical printing, which has long made its way into most people’s homes. 3D printing on the macroscale was presented by Swainson² and Hull³, almost 50 years ago. Swainson already realized the importance of nonlinearities. Using stereolithography, Kodama⁴ realized early on 3D polymer structures. 3D additive manufacturing on the micro- and nanoscale was first realized experimentally in the 1990s by Maruo and coworkers⁵. Herein, negative-tone photoresists were processed by a nonlinear optical multi-photon-based technique.

Correspondence: Martin Wegener (martin.wegener@kit.edu)

¹Institute of Nanotechnology, Karlsruhe Institute of Technology (KIT), 76128 Karlsruhe, Germany

²Institute of Applied Physics, Karlsruhe Institute of Technology (KIT), 76128 Karlsruhe, Germany

Full list of author information is available at the end of the article.

© The Author(s) 2021



Open Access This article is licensed under a Creative Commons Attribution 4.0 International License, which permits use, sharing, adaptation, distribution and reproduction in any medium or format, as long as you give appropriate credit to the original author(s) and the source, provide a link to the Creative Commons license, and indicate if changes were made. The images or other third party material in this article are included in the article's Creative Commons license, unless indicated otherwise in a credit line to the material. If material is not included in the article's Creative Commons license and your intended use is not permitted by statutory regulation or exceeds the permitted use, you will need to obtain permission directly from the copyright holder. To view a copy of this license, visit <http://creativecommons.org/licenses/by/4.0/>.

In this review, we focus on multi-photon approaches which have seen a rapid recent development. Multi-photon approaches include two-photon absorption as well as the use of more than two photons in the excitation process. Today, multi-photon approaches provide printing rates of up to about ten million voxels per second⁶. To illustrate the meaning of this speed, we mention in passing that commercial home office 2D inkjet printers operate at rates of nearly ten million pixels per second. The consumer perceives these speeds as sufficiently fast. Multi-photon-based 3D approaches structure matter with a resolution approaching sub-micrometer and nanometer feature sizes^{7,8}. Such spatial resolution is crucial for many applications in photonics and electronics^{9–12} and is inaccessible to most other 3D additive manufacturing approaches⁶. However, the vast majority of 3D printed objects and devices made along these lines has been composed of only a single polymeric material. Multi-material architectures are much less investigated than single-material architectures, yet, most real-life systems (microscopic and macroscopic, biological and artificial) contain a large number of different materials with vastly dissimilar optical, mechanical, thermal, and electronic properties. Just consider the ingredients of a modern mobile phone. Therefore, this review further focuses on multi-material multi-photon approaches.

The main challenge starts with the correct “primary materials” in analogy to the primary colors. For example, electrically conducting or semiconducting primary materials cannot be obtained by combination of any number of non-conductive polymers. Here we review existing materials that might serve as a working set of “primary materials”. In the second step, we discuss processing dissimilar primary materials within 3D printed structures using a single machine tool. We divide the corresponding literature into two avenues.

In the first avenue, different photoresists – the counterparts of the colored inks – are combined to manufacture a targeted multi-material 3D structure. So far, this combination has been accomplished by intermediate manual processing steps, but automated multi-photon multi-material 3D printing systems are rapidly developing.

In the second avenue, a *single* photoresist delivers 3D printed material with different properties. There is no direct analogue in graphical 2D printing. The underlying idea is to impose a stimulus during the 3D printing process of each voxel, influencing the photo-reaction of the ink, such, that the emerging material properties can be varied locally and deterministically in 3D. Conceivable stimuli include the locally applied laser power (e.g., changing the polymer cross-linking density), a quasi-static electric field vector

(e.g., aligning molecules with an electrical dipole), a magnetic-field vector (e.g., aligning magnetic dipoles), or the wavelength of the exciting light (e.g., initiating reactions of different components within a single fixed photoresist system). A single, highly optimized “ink”, delivered to the printing zone (defined by the laser focus), creates highly resolved multi-material 3D objects. This concept can of course be expanded to multiple photoresists. This review presents the current state-of-the-art of multi-material multi-photon 3D laser printing.

However, in this review, we will not cover the far-reaching idea of 3D metamaterials or “meta-inks”. Printing 3D metamaterials mimics dithering in 2D graphical printing. We refer the reader to recent review articles by us^{7,13} and others^{14,15}. Nature proceeds quite similarly. It achieves a vast variety of different effective material properties in animals and plants by architecting on a micrometer and nanometer scale by using only a limited number of building blocks, based on polysaccharides, proteins, and minerals¹⁶. Printing tailored 3D microstructures results in artificial composites, with effective optical, mechanical, thermal, and electronic properties that can be qualitatively dramatically distinct from those of the constituents. As for dithering in 2D, it is key that the characteristic feature sizes are sufficiently small such that the observer does not notice them and rather experiences an effective homogeneous continuum (analogous to a homogeneous color).

Multi-photon 3D laser printing

In multi-photon 3D laser printing (alternatively 3D laser lithography or 3D direct laser writing), one tightly focuses laser pulses into the volume of a photosensitive material, the photoresist. Multi-photon absorption restricts the excitation to the focal region only and avoids spillover effects common and unavoidable in one-photon absorption¹⁷. The shape of the focal volume – locus of the chemical reaction – can also be influenced by the light’s polarization¹⁸. The nature of this chemical reaction can differ greatly. For example, in monomers, light induces a local cross-linking^{19,20}. In metal salts, light induces a reduction leading to metal nanoparticles in solution²¹. By scanning the laser focus through the photoresist in three dimensions, the desired 3D architecture is defined, including the possibility of overhanging structures. We note that, unlike for other 3D additive manufacturing approaches, a supporting material is usually not needed to realize overhangs. For example, to 3D print a bridge, layer-by-layer approaches need to print something underneath the bridge because material cannot be deposited onto air. After the printing process, the auxiliary material needs to

be removed. Multi-photon 3D laser printing does not require such auxiliary materials as the polymerized part “swims” in the liquid monomer surrounding. Using galvanometric mirror scanners, focus speeds of up to about half a meter per second at sub-micrometer voxel sizes have been reported⁶. Scanning of the illumination with speeds approaching the vacuum velocity of light is possible by projection-based temporal focusing²². After writing is completed, a suitable solvent removes the unexposed parts. The chemistry and mechanism involved in the printing processes depends on the photoresist system^{17,19,20}. However, even for the most investigated monomer-based photoresist systems, details of the reaction-diffusion kinetics in three dimensions are not well understood. The situation is yet less clear for metal salts as photoresists for 3D printing of noble metals.

Primary material properties from multi-photon photoresists

Bulk polymers:

Commonly used photoresists are composed of a monomer, a cross-linker, a photoinitiator, a photoinhibitor, and a solvent. By tightly focused laser irradiation, the monomer rapidly and efficiently crosslinks into a bulk polymeric network^{19,20}. Inks can be acrylate-based (e.g., IP series, Nanoscribe GmbH), epoxy-based (e.g., SU-8 series, MicroChem), organic-inorganic hybrids (OrmoComp, MicroResist Technology), or hydrogel-forming photoresists^{23–27}. Many photoresists are commercially available and ready-to-use without complicated preparation, enabling rapid fabrication of mechanically and chemically stable structures. The mechanical, thermal, optical, and bio-compatible properties of these materials allow the design of unique functional structures for applications as cell scaffolds^{28,29}, 3D metamaterials^{30–33}, microoptical elements^{34–36}, microrobots^{37–39}, and functional surfaces^{40–42}. Bulk photoresists can be mixed with inert polymers such as Poly(methyl methacrylate) (PMMA) to customize properties, leading for example to better mechanical strength and higher viscosity in the manufacturing of overhanging structures⁴³.

Conductive polymers:

The efficient multi-photon 3D printing of conductive polymers is an open challenge. Due to the strong absorption in the near-infrared, many intrinsically conductive polymers which can be used in other 3D printing techniques are difficult to use in multi-photon polymerization processes⁴⁴. Poly (3,4-ethylenedioxythiophene) (PEDOT) and its relatives are attractive for

electronic applications because of their high conductivity and stability. PEDOT also is biocompatible and allows its use in biological environments⁴⁵. Multi-photon 3D laser printing by in situ oxidative polymerization of EDOT mixed in polyethylene glycol diacrylate⁴⁶ or by polymerization of an EDOT-dimer⁴⁷ were demonstrated. Another important conducting polymer is polypyrrole. Polypyrrole (Ppy) and its derivatives have been studied intensely in different fields such as sensing or batteries^{48,49}. Ppy displays high conductivity, and environmental stability even in the presence of liquid electrolytes. Unfortunately, truly 3D laser printing of this polymer has not been realized yet. An important step into this direction was taken by Agarwal et al. They demonstrated the use of a femtosecond laser as a new method for the polymerization and patterning of Ppy. In particular, pyrrole-3-carboxylic acid (PCA), was used for the writing of conductive patterns within microchannels. Its higher water solubility leads to favorable adhesion to glass surfaces. A conductivity of $1.7 \times 10^3 \text{ Sm}^{-1}$ has been measured from a PCA polymer pattern⁵⁰.

Metals:

The high optical peak intensities occurring within the focal volume of multi-photon 3D printers also allow direct photo-reduction of metal salts into metallic micropatterns with nanoscale precision²¹. Here, the photoresist is usually composed of a metal salt, a photosensitizer, a reducing agent, and surfactants. All of these components are dissolved in water or in a polymer matrix. Silver^{51,52} and gold salts^{53,54} are popular, but noble metals such as platinum and palladium have also been reported^{55,56}. The direct laser writing of metal patterns has led to promising applications in microelectronics⁵³, sensing and detection⁵⁷, microfluidics⁵⁸, and split-ring resonators for optical metamaterials⁵⁹.

Nanoporous polymers:

A porogen is a chemically inert component which is miscible with the photoresist in its unpolymerized state, but induces a phase separation after multi-photon exposure resulting in porous structures. Importantly, separated phases may not display a large refractive-index contrast. Otherwise, light is scattered during the printing process. During development, the porogen is washed out from the pores and a nanoporous and strongly light-scattering structure emerges⁶⁰. Such nanoporous 3D printed architectures have potential applications in controlling diffuse light scattering, as nanoparticle filters in microfluidics, as super-hydrophobic surfaces, or as scaffolds for cell and tissue culture.

Glasses:

Many polymers have refractive indices in the range of $n = 1.5$ and no polymer exceeds $n = 1.7$. While such values suffice for many applications in optics, e.g., for microlenses and photonic wire binds⁶¹, tight waveguide bends or 3D photonic-band-gap architectures require larger refractive-index contrasts. A number of inorganic materials, such as chalcogenide glasses, PbSe, and LiNbO₃, has sufficiently large refractive indices and 3D structures have successfully been made via direct multi-photon laser printing^{62–64}. An alternative is to mix inorganic nanoparticles into monomeric photoresists. Examples are silicon-based monomers mixed with zirconium acrylate and titanium acrylate^{65,66}. In these approaches, the refractive index can be tailored by the composition. More recently, the Rapp group demonstrated two-photon 3D printing of fused silica glass⁶⁷. Their photoresist contained 32.5 vol% silica nanopowder in a photocurable binder matrix consisting of 40 vol% hydroxyethyl methacrylate and 60 vol% of trimethylolpropane ethoxylate triacrylate as crosslinker. After the 3D printing process, the structures were sintered at temperatures up to 300 °C to obtain pure silica glass. Related processes have recently also been published by other groups^{68,69}.

Crystals:

Optically transparent micro- and nanostructures have also been accomplished by using Yttrium-Aluminium-Granat (YAG) crystals as a solid photoresist in the sense that the crystal has been exposed to light^{70,71}. Following light exposure, selective etchants are used to produce voids within the YAG crystal. This ansatz is conceptually similar to that used in chalcogenide glasses (see previous section)⁶².

Natural polymers:

Many polymers discussed above and others have successfully been used for the preparation of extracellular bio-scaffolds to support and interact with living mammalian cells⁷². An interesting alternative are proteins as photoresists. By multi-photon polymerization of proteins, specific cell-affinity has been realized⁷³. Bovine serum albumin (BSA)²⁶ is crosslinked when Rose Bengal is used as photosensitizer. However, the mechanical properties of cross-linked proteins are inferior to those of polymers. In addition, they have to be kept in a buffer solution to maintain their shape. Gelatin, a widely available biopolymer, can overcome many of these issues⁷⁴. Different groups have assembled 3D structures using gelatin and its derivatives⁷⁵. Besides BSA and gelatin, other proteins and biomacromolecules, have been used as well,

including chitosan, avidin, biotin, and fibrinogen^{76–78}.

Stimuli-responsive materials:

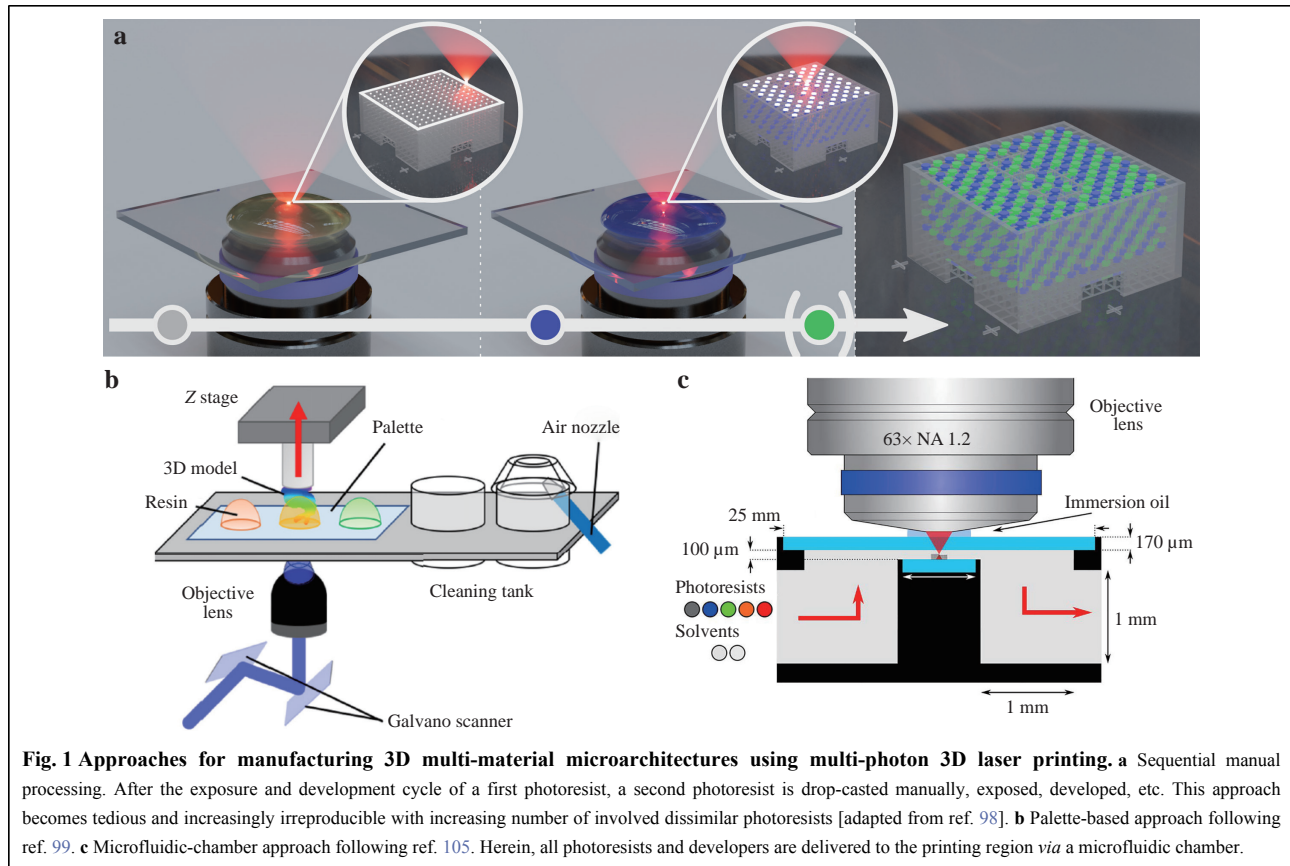
3D printable stimuli-responsive polymers, hydrogels, and organogels emerge as an important and growing class of materials that are only covered as stimuli-responsive ingredients here (Section of multi-material stimulus-responsive microrobotics), as the topic has been reviewed recently⁷⁹.

Polymer composites:

Many polymers discussed above and others have successfully been used for the preparation of extracellular bio-scaffolds to support and interact with living mammalian cells⁷². An interesting alternative are proteins as photoresists. By multi-photon polymerization of proteins, specific cell-affinity has been realized⁷³. Bovine serum albumin (BSA)²⁶ is crosslinked when Rose Bengal is used as photosensitizer. However, the mechanical properties of cross-linked proteins are inferior to those of polymers. In addition, they have to be kept in a buffer solution to maintain their shape. Gelatin, a widely available biopolymer, can overcome many of these issues⁷⁴. Different groups have assembled 3D structures using gelatin and its derivatives⁷⁵. Besides BSA and gelatin, other proteins and biomacromolecules, have been used as well, including chitosan, avidin, biotin, and fibrinogen^{76–78}.

Multiple material properties from multiple photoresists

The sequential 3D printing of dissimilar photoresists – as described in the preceding section – appears as a simple and straightforward approach to fabricate multi-material 3D structures: After exposing and developing a first photoresist, a second photoresist is introduced and exposed, developed, etc. This procedure is illustrated in Fig. 1a. Herein, positioning accuracy is of utmost importance⁸⁶. Yet, a couple of fundamental restrictions apply. For example, after 3D printing dense metal or metal containing parts, the architecture is no longer transparent to light. Furthermore, it scatters the incident light. Both aspects make subsequent controlled multi-photon exposures difficult. Even if all previously 3D printed components are optically transparent, caution has to be exerted. If, for example, the different components have dissimilar refractive indices, the resulting laser focus is prone to optical aberrations, leading to distortions of the position as well as the size of subsequently 3D printed voxels. The strength of these aberrations depends on the refractive-index contrast and on the thickness the light has to pass towards the focus. In principle, in analogy to optical



microscopy, these optical phase aberrations can be pre-compensated by using a spatial phase modulator. This would require knowledge of the spatial refractive-index distribution or algorithms for compensation without such knowledge^{63,87}. However, so far, such corrections have not been applied in the context of multi-material multi-photon 3D laser printing. In addition, good adhesion between the different printed materials is required for the integrity of the final 3D structure. Although this is usually not an issue when using polymeric photoresists due the presence of unreactive groups in the surface of the pre-printed structures which allow the formation of covalent bonds in the next printing step, it can be challenging when combining materials with very different properties and nature, e.g., metals and polymers or organic and inorganic materials.

Given these constraints, the following multi-material systems have been developed. Applications in biology, optics and photonics, responsive microrobotics, and microelectronics have been achieved.

Methods and systems for the assembly of multiple materials

One option is to perform the steps mentioned above and

depicted in Fig. 1a manually^{88–95}. Most published multi-material 3D structures made this way are composed of merely two dissimilar photoresists and only few samples have been reported to be composed of more than 2 kinds of materials^{92,96–98}. However, with increasing number of different photoresists, this approach tends to become terribly difficult and irreproducible because the previously printed structure must be realigned manually in each step. This has spurred the recent development of different automated systems capable of 3D printing multi-material architectures.

A first approach is illustrated in Fig. 1b. It is based on storing the different photoresists and solvents on a surface or plate that can be moved by an automated linear or a rotational stage^{99–102}. To avoid contamination between the different materials, two cleaning tanks containing solvents are included. In addition, an air nozzle allows for cleaning and drying. Although one-photon absorption in the ultraviolet is used here, this approach could be translated to multi-photon polymerization.

The second approach is based on integrating microfluidics into the 3D laser printer. Sun's group attached a polydimethylsiloxane (PDMS) parapet onto a glass substrate to form a microfluidic chip for flexible

injection and emission of photoresists and developer. This on-chip multi-photon polymerization strategy allows in-situ integration of multiple photoresists. Microrobots and actuators have been demonstrated by combining rigid and stimuli-responsive resists¹⁰³. Lamont et al. introduced a vacuum system to perfuse the PDMS-glass microchannel with liquid-phase photocurable material or developer. Along these lines, a DNA-inspired microstructure with five different materials has been achieved¹⁰⁴. The positioning errors for the different materials have been on the 100 nm level.

Mayer et al. integrated a reusable microfluidic chamber into a state-of-the-art commercial 3D laser printing system (cf. Fig. 1c). The chamber was connected to customized pressure-flow control units. Seven different liquids, including five photoresists and two solvents, were used. However, the approach can easily be scaled up to a larger number¹⁰⁵. Microfluidic devices also allow to polymerize multiple materials simultaneously when multiple photoresists are injected at the same time^{106,107}.

Multi-material systems for applications in biology

Tailored 3D scaffolds influence and direct proliferation, migration and maturation of different cell types⁷². To resolve more complicated biological questions, 3D scaffolds composed of multiple materials and different surface functionalities are required. Sequential processing gives scaffolds with distinct protein-binding and protein-repellent properties (Fig. 2a). Selective cell adhesion sites on scaffolds provide control of cell adhesion and cell shape in three dimensions⁸⁹. Specific functional sites can be realized by photoinduced selective grafting of maleimide and subsequent bioconjugation. In this method, a homogeneous topography without discernible topographical change can be maintained¹⁰⁸. Based on the control of cell shape and growth with well-defined adhesion sites in 3D (Fig. 2b, c), quantitative image processing and mathematical modeling reveal that the fibroblast shape is not only determined by contractility, but also by elastic stress in the peripheral actin bundles¹⁰⁹. With 3D scaffolds defining the shape of cells, external forces can be applied to specific adhesion sites of single cells, enabling quantitative statistical analysis¹¹⁰. As mentioned above, proteins are interesting in this context. However, it is difficult to stack extracellular matrix proteins, such as fibronectin, to fabricate 3D scaffolds extending over 100 μm . Sie et al. adopted a multi-material approach based on BSA in a first step. In a second step, human fibronectin was inserted at specific locations (Fig. 2d)⁹⁰. Proteins can also be embedded into a photoresist microstructure to increase the mechanical robustness of free-standing 3D

protein microstructures^{111,112}. Serien et al. demonstrated proteinaceous networks within one microstructure¹¹¹. By sequentially processing of different materials, 3D scaffolds with more than 2 constituents are possible (Fig. 2e, f). The combination of a protein-repellent photoresist with a protein-adhesive resist as well as a photoactivatable passivating resist has been demonstrated^{91,92}. Selected domains of these structures can be addressed by two distinct proteins (Fig. 2f).

Incorporation of responsive materials into bio-scaffolds facilitate the active response of scaffolds to tailored 3D microenvironments¹¹³. In this study, protein-repellent trimethylolpropane ethoxylate triacrylate (TPETA) was used for walls; pentaerythritol triacrylate (PETA), which adheres proteins on its surface, as the beams, and most importantly, stimuli-responsive host-guest hydrogel as actuator cell stretching (Fig. 2g-i) – in essence a micro-stretch-bench for cells.

Multi-material systems for optics and photonics applications

2D fluorescent security features are ubiquitous, e.g., on Euro bank notes and certain passports. Going to three dimensions increases counterfeit security. Different colors corresponding to different photoresists are needed. An early demonstration was based on polymers doped with fluorescent semiconductor quantum dots⁹⁸. 3D laser printing provides more security against counterfeiting compared with 2D structures. The combination of multiple fluorescent materials allows complicated optical patterns to be embedded. Herein, a nonfluorescent photoresist (PETA) served as a cross-grid holder structure. Onto this holder, two different fluorescent photoresists containing semiconductor quantum dots with fluorescence emission wavelengths of 525 and 450 nm, respectively, were 3D printed. Finally, the 3D structure was encapsulated in PETA, resulting in a thin transparent polymer film with fluorescent markers in its interior. Early structures were manufactured manually (see above). Later¹⁰⁵, the described microfluidic system described has been used for the 3D printing of security features containing 5 different ingredient materials (Fig. 3a).

Multiple materials are also needed for correcting chromatic aberrations of microoptical components. Using two different photoresists (IP-S and IP-Dip) with different refractive indices, an achromatic axicon and a Fraunhofer doublet were fabricated by the Giessen group¹¹⁴. The same group also demonstrated the integration of polarization control (IP-Dip used for high resolution) and focusing elements (IP-S used for low shrinkage) directly onto the end facet of an optical fiber (Fig. 3b)¹¹⁵. Such components

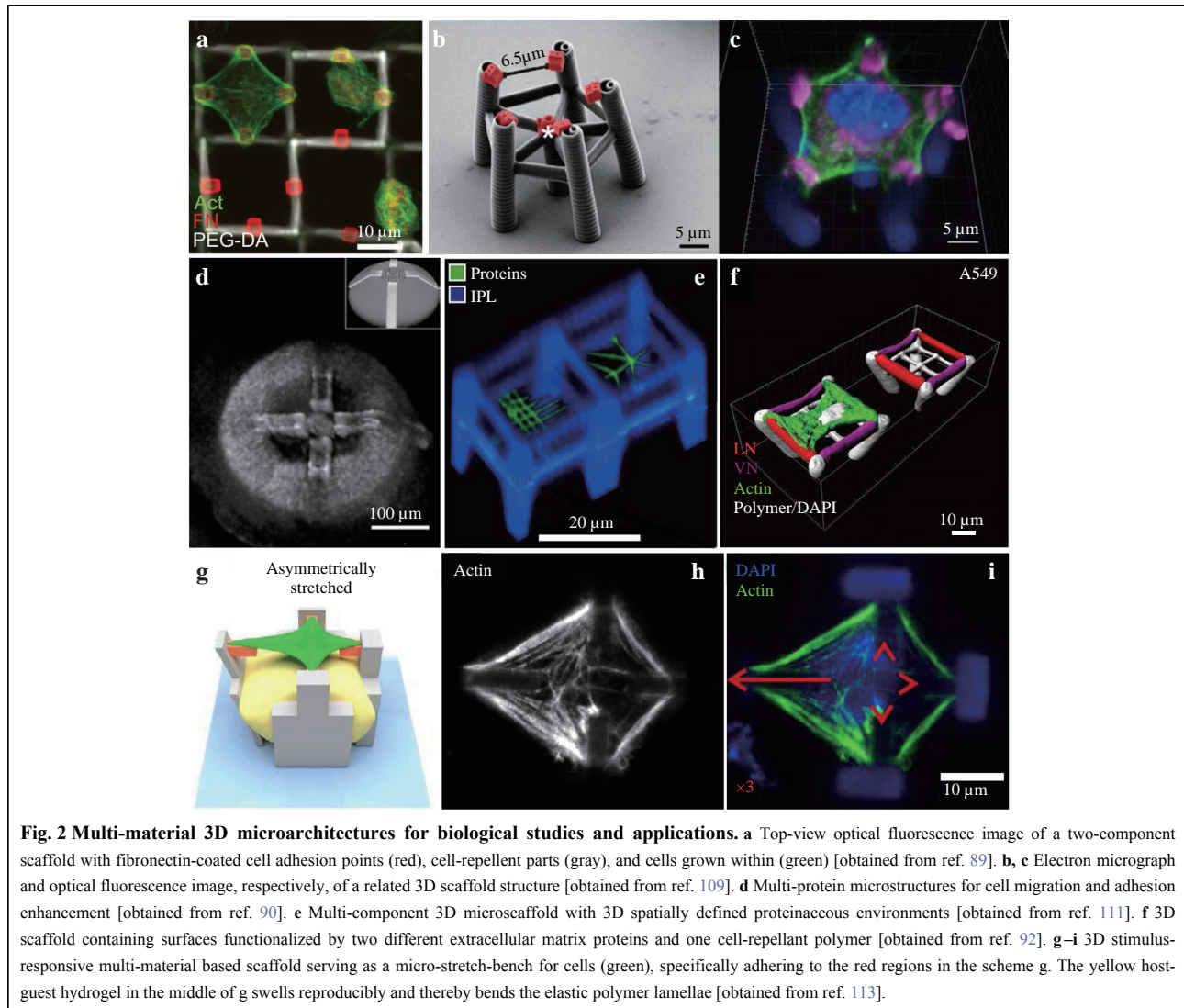


Fig. 2 Multi-material 3D microarchitectures for biological studies and applications. **a** Top-view optical fluorescence image of a two-component scaffold with fibronectin-coated cell adhesion points (red), cell-repellent parts (gray), and cells grown within (green) [obtained from ref. 89]. **b, c** Electron micrograph and optical fluorescence image, respectively, of a related 3D scaffold structure [obtained from ref. 109]. **d** Multi-protein microstructures for cell migration and adhesion enhancement [obtained from ref. 90]. **e** Multi-component 3D microstructure with 3D spatially defined proteinaceous environments [obtained from ref. 111]. **f** 3D scaffold containing surfaces functionalized by two different extracellular matrix proteins and one cell-repellant polymer [obtained from ref. 92]. **g–i** 3D stimulus-responsive multi-material based scaffold serving as a micro-stretch-bench for cells (green), specifically adhering to the red regions in the scheme **g**. The yellow host-guest hydrogel in the middle of **g** swells reproducibly and thereby bends the elastic polymer lamellae [obtained from ref. 113].

can also be directly 3D printed onto the end facets of light-emitting diodes and onto optical chips.

By integrating stimuli-responsive materials, tunable optical systems become accessible. The Wiersma group designed, 3D printed, and characterized an integrated polymeric photonic circuit with waveguides, grating couplers, and ring resonators in a dense geometry^{116,117}. The waveguides and grating couplers were made from rigid commercial IP-Dip photoresist (Nanoscribe GmbH), while the ring resonator was made from and actuated by a liquid-crystal elastomer. Light served as a stimulus to spectrally tune the response of the photonic circuit in a controlled and reversible manner (Fig. 3c).

Multi-material stimulus-responsive microrobotics

Responsivity is crucial for accomplishing tasks such as environmental remediation¹¹⁸, cargo transportation⁸², and

therapeutics in confined spaces⁸⁴. The most used stimuli-responsive materials in multi-photon 3D laser printing are hydrogels/organogels, which change their volume under stimuli, e.g., pH value⁷⁷ or temperature¹¹⁹. To achieve complex actuation, the fabrication of multi-material structures is required. Often, responsive and non-responsive (passive) materials are combined.

A representative example is BSA-based hydrogel. At isoelectric pH, the BSA proteins are uncharged and assume their lowest volume. Once the pH value is changed, the protein chains become ionized because of deprotonation/protonation of the amino acid groups. The strong electrostatic repulsion between the BSA molecular chains leads to the swelling of the BSA structure. Sun's group developed a successive on-chip 3D laser printing strategy to distribute BSA and SU-8, which act as muscles and skeletons in 3D musculoskeletal systems¹⁰³. The

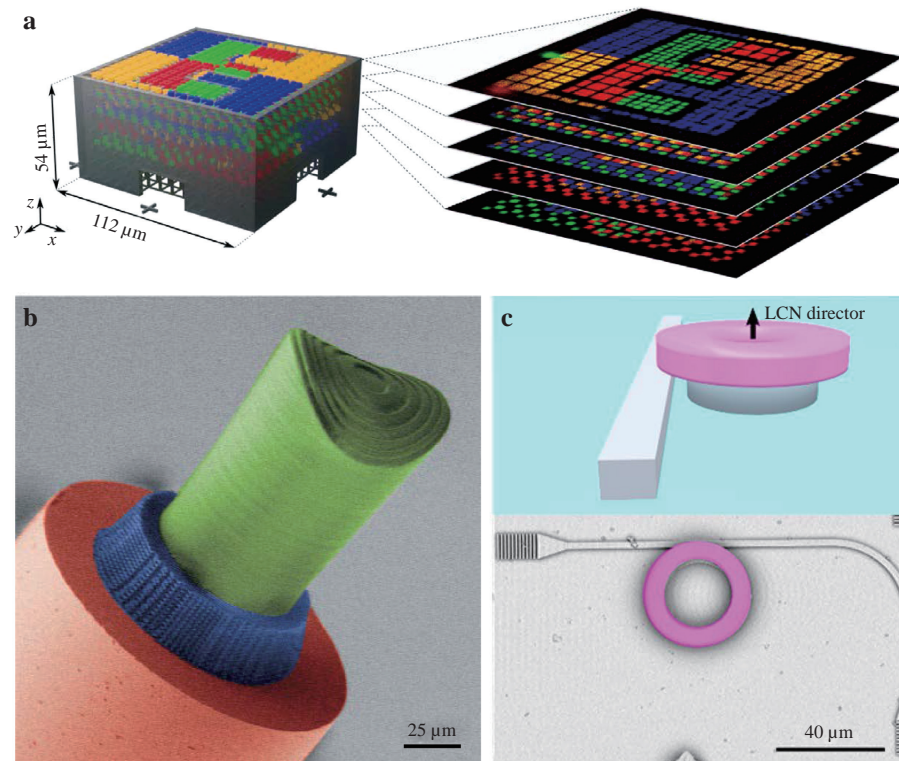


Fig. 3 Multi-material 3D microarchitectures for applications in optics and photonics. **a** Left: Scheme of a 3D deterministic fluorescent security feature containing four differently doped polymers emitting at four different wavelengths (red, blue, green, and yellow) and one non-fluorescent polymer component. Right: Measured fluorescence stack [obtained from ref. 105]. **b** Colored electron micrograph. A microoptical lens composed of two different polymers (blue and green) has directly been 3D printed onto the end facet of a single-mode optical fiber (red) [obtained from ref. 115]. **c** Polymer waveguide on a substrate and ring liquid-crystal elastomer optical ring cavity. By stimuli such as temperature and light, the liquid-crystal elastomer swells/contracts, allowing for tuning the coupling between waveguide and resonator [obtained from ref. 116].

internal network of both BSA and SU-8 can be programmed at the microscale and the elasticity of the muscle as well as the stiffness of the skeleton can be tuned for flexible actuation. On this basis, a pH-responsive spider microrobot was realized (Fig. 4a, b). In addition, a crab claw-muscle system and a smart microgripper were fabricated, which allows for pH-controlled capturing and releasing of microtargets. All of these musculoskeletal structures exhibit fast response, good durability, and robustness after long-time storage.

Temperature is another important stimulus parameter. Poly(N-isopropylacrylamide) (pNIPAM) is a well-established polymer, exhibiting a substantial response to changes in temperature due to its lower critical solution temperature. Employing pNIPAM, Hippler et al. designed micrometer-scale rigid tubes with stimuli-responsive valves. The main body of the tubes was fabricated by PETA. A pNIPAM-based torus was written inside the tube as a valve. By changing the temperature between 45°C and 20°C, the cross section of the tube was changed by a factor

of 2.5¹¹⁹. pNIPAM can also act as a supporting platform for the successive writing of IP-L photoresist. In this way, freely suspended microstructures of a second material like a skeleton can be inscribed into a temperature-responsive pNIPAM matrix¹²⁰. Nishiyama et al. deposited Ag nanoparticles inside temperature-responsive pNIPAM microgels. By their plasmonic absorption resonance, the Ag nanoparticles efficiently convert light into heat, leading to reversible relative microgel volume changes as large as 86%¹²¹.

Another mechanism is solvent-induced swelling of a hydrogel in a network with rigid materials. Duan's group presented a solvent-responsive hydrogel, which consisted of acrylamide as monomer and the sodium salt of 2-acrylamido-2-methylpropane sulfonic acid as the ionic comonomer for the 3D printing of a micropump. This micropump system comprised a microfluid channel out of a passive photoresist (SCR 500) and a responsive hydrogel film as valve. By alternating the solvent composition (ethanol/water), the hydrogel film bent and led to

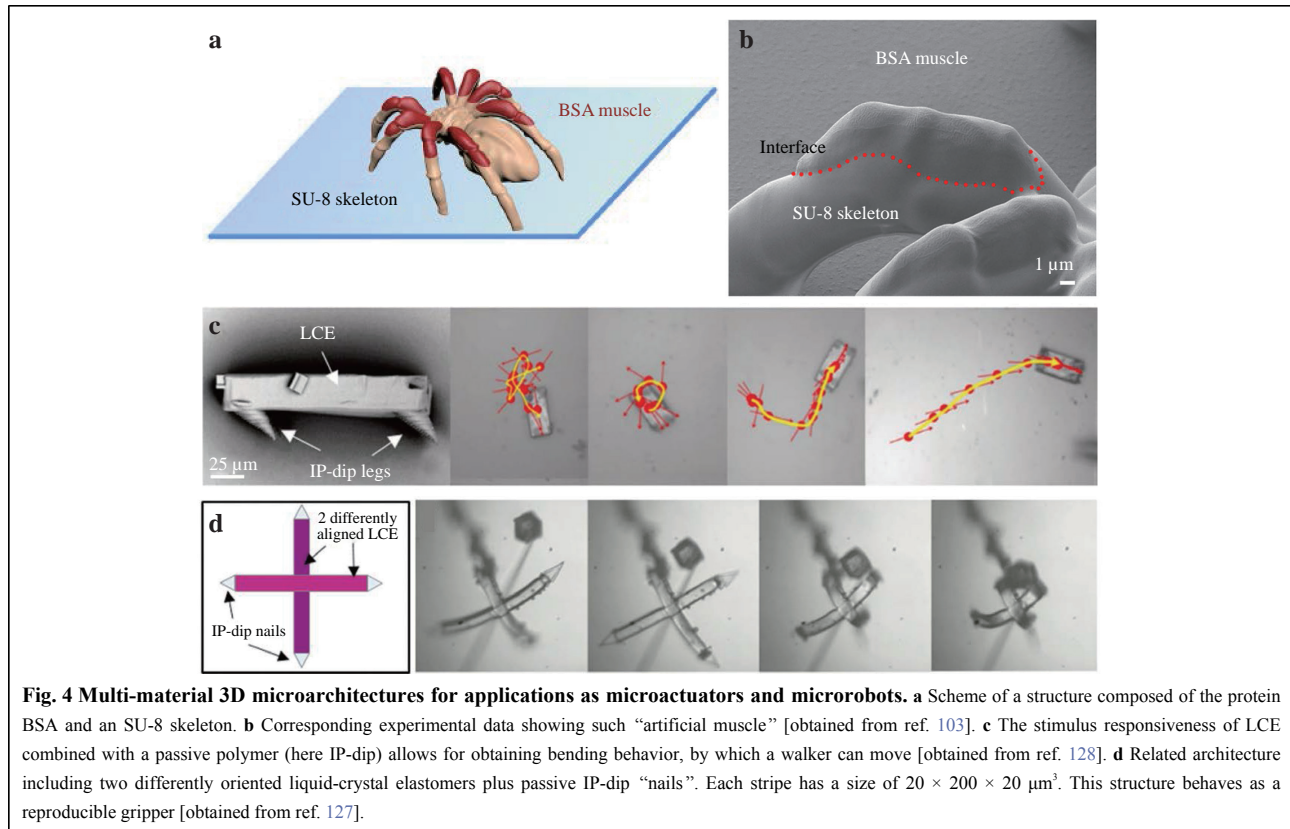


Fig. 4 Multi-material 3D microarchitectures for applications as microactuators and microrobots. **a** Scheme of a structure composed of the protein BSA and an SU-8 skeleton. **b** Corresponding experimental data showing such “artificial muscle” [obtained from ref. 103]. **c** The stimulus responsiveness of LCE combined with a passive polymer (here IP-dip) allows for obtaining bending behavior, by which a walker can move [obtained from ref. 128]. **d** Related architecture including two differently oriented liquid-crystal elastomers plus passive IP-dip “nails”. Each stripe has a size of $20 \times 200 \times 20 \mu\text{m}^3$. This structure behaves as a reproducible gripper [obtained from ref. 127].

reversible absorption and discharge of the fluid¹²². Another hydrogel prepared from butyl methacrylate as a monomer and propoxylated trimethylolpropane triacrylate as a cross-linker was used for the fabrication of a slipping-block microdevice¹²³. Sun’s group combined a humidity-responsive polyethylen glycol diacrylate (PEG-DA) hydrogel and inert methacrylate-based material using a two-steps fabrication method. A directionally bending cantilever was accomplished based on a hydrogel part swelling or shrinking in response to humidity changes²⁵.

Liquid-crystal elastomers (LCEs) represent another class of stimuli-responsive materials that are multi-photon printable¹²⁴. For an introduction to the working principle and composition of LCEs, we refer the reader to ref. 125. Note that, in contrast to ordinary polymers, LCEs exhibit a preferred axis commonly referred to as the director. Raising the LCE temperature from below to above their phase-transition temperature, LCEs perform a phase transition from anisotropic medium to an isotropic medium. Various 3D movements, such as bending, contraction, torsion, jumping, and rotation of LCE can be reversibly controlled by programming the LCE director. These movements are triggered by various stimuli such as temperature, light, pH value, and electric or magnetic fields^{126,127}. Wiersma and co-workers have reported a series

of multi-material microactuators made by multi-photon 3D printing of LCEs and ordinary photoresists. A first example is a microscopic walker, which is able to move on different substrates in a dry environment¹²⁸. Its main body was made from LCEs, which act as muscles (see Fig. 4c), and the four conical legs were made using IP-Dip photoresist. More recently, a hominid inspired microhand composed of four LCE fingers and four IP-Dip nails was realized¹²⁹. Two of the fingers have different molecular alignment compared to the other two and bend in different directions under optical illumination. This microhand grabs and holds small objects when illuminated by green laser light without specific requirements for the environment (see Fig. 4d).

Multi-material 3D structures for microelectronics

For microelectronics, electrically conductive structures are crucial. As discussed above, various metals have been printed via multi-photon induced reduction of metal salts. However, it has so far proven difficult to obtain complex 3D structures along these lines^{51–53,130,131}.

In a first approach, photoresists with different functional groups are printed sequentially. Thereafter, the entire structure is selectively coated with metal layers due to the difference in functional groups. Using this approach, the Kawata group reported the fabrication of 3D

silver/polymer conjugated microstructures⁸⁸. Herein, photopolymerizable photoresists with and without an amide group were independently prepared. Using electroless plating, silver was selectively deposited on the surface of the amide-containing polymer parts (Fig. 5a). The Fourkas group demonstrated the selective chemical functionalization of 3D polymer microstructures composed of an acrylic polymer and a methacrylic polymer in different parts¹³². The microstructures were rinsed in an ethylenediamine solution. A highly selective Michael addition occurs only on the unreacted acrylate surface, leaving free amines on the surface of the acrylic portion of the structures but not on the methacrylate regions. Finally, the acrylic regions were selectively coated with Au and Cu, respectively (Figs. 5b–d).

In a second approach, ordinary polymer structures serve as the 3D scaffolds for the printing of metallic structures. The Fourkas group reported laser writing of silver lines from a poly(vinylpyrrolidone) (PVP) thin film containing silver nanoparticles as silver cations. After printing of the

polymer structure, a PVP layer was coated on its surface, followed by laser writing. In this fashion, 3D metal lines on dielectric polymer structures were realized¹³³.

As discussed above, the most common approach to obtain metals by multi-photon 3D laser printing is by photoreduction of metal salts from aqueous solution. The water can also be replaced by a hydrogel, acts both as a container and 3D supporter for metal reduction (see Fig. 5e)¹³⁴.

As an original part of this review article, we have recently realized the fabrication of isolated metal cables and truly 3D metal lines. First, 2D or 3D polymer substrates have been written by using the (electrically isolating) PETA photoresist. After development, the structure was exposed to aqueous ammonium tetrachloroplatinate⁵⁵. Second, platinum lines were printed on the resulting surfaces (or on the glass substrate surface). A continuous 3D platinum line running over a PETA bridge is shown in Fig. 5g. As the laser impinges through the glass substrate, the refractive index of which is roughly

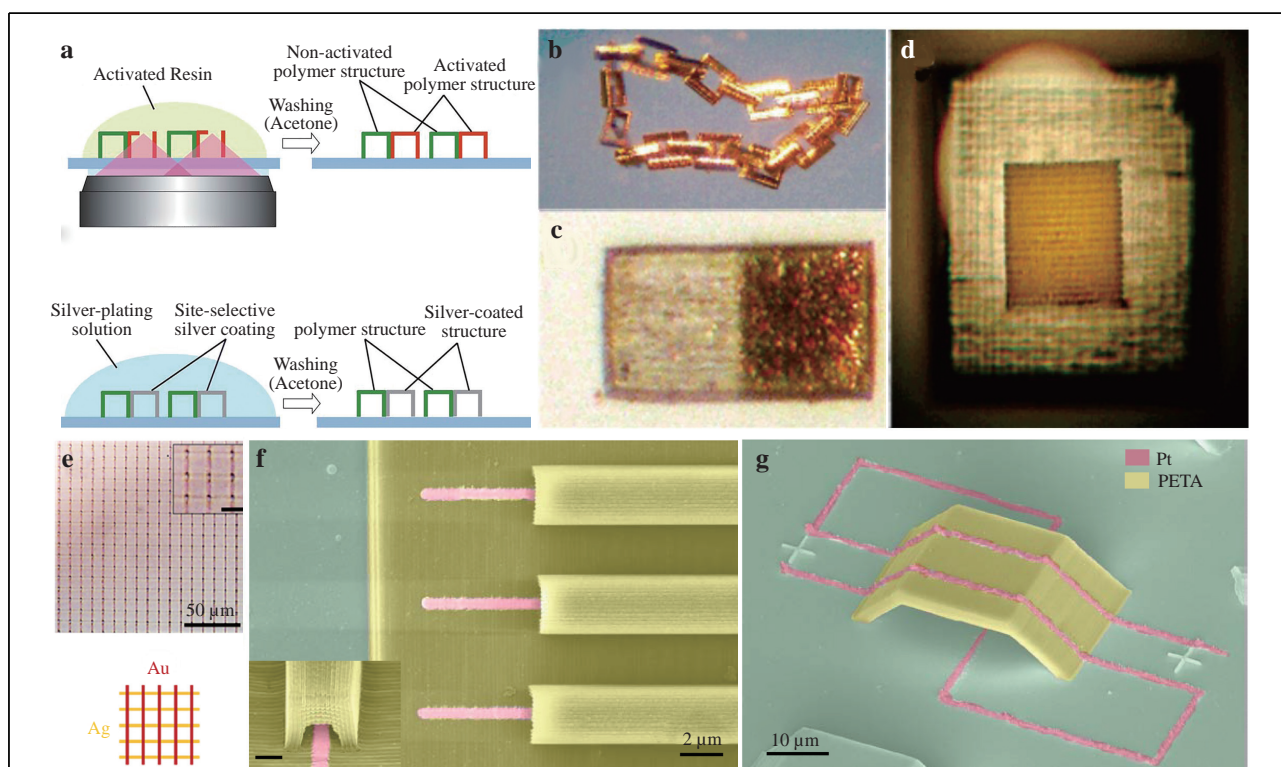


Fig. 5 Multi-material 3D microarchitectures including conductive parts for applications in microelectronics. **a** Side-by-side silver-coated and bare polymer horseshoe structures made by selective electro-less plating of two different polymers [obtained from ref. 88]. **b–d** Examples for selectively copper-coated 3D structures. Each link in **b** is 70 μm long. Adjacent polymer squares in **c** are 20 μm on a side [obtained from ref. 132]. **e** Cross-grid structure manufactured by multi-photon induced-reduction of two different metal salts in a hydrogel. The vertical lines (red) are made out of gold, the horizontal ones (yellow) out of silver [obtained from ref. 134]. **f, g** Colored electron micrographs of two different 3D hetero microstructures composed of an electrically isolating polymer (PETA, yellow) and conductive platinum (pink) made by multi-photon reduction. The structure shown in **f** can be seen as an isolated electrical cable on the micrometer scale. The structure in **g** demonstrates that the electric wires can be guided towards the third dimension by using an ordinary polymer as support structure. Original results by the authors of this paper.

that of the aqueous solution, metal lines can be printed underneath the polymer bridge as well as on top of it. Here we have used a water-immersion microscope objective lens (Zeiss, LD C-Apochromat 63x/1.15). The metal can also be isolated electrically to form a microcable (Fig. 5f). Here, a small gap between the metal and the polymer has developed due to polymer shrinkage. Such electrically isolated structures might be useful for applications in which the cable is used in an electrolytic environment, where contact of the metal line to the environment is unwanted. However, the shrinkage-induced gap would have to be filled-in by an additional lithography step to avoid electrical short circuits.

Multiple material properties from a single photoresist

Multiple material properties can be obtained by applying a stimulus to a given dedicated photoresist during the 3D printing process. The underlying principle is that the stimulus influences the multi-photon-absorption induced chemical reactions such that the emerging material properties can be determined locally in 3D. Here, we review the few examples in the literature which have used this approach.

The simplest possibility to control the material properties is to change the monomer cross-linking density by changing the laser exposure dose. The latter can be realized by changing the incident laser power, the focus scanning speed, by multiple exposures (connected to the hatching and slicing distance), or by combinations of these. This approach has also been coined gray-tone lithography. An example for a parameter that can be changed significantly along these lines is the thermal expansion coefficient of the polymer³¹. A single photoresist (IP-Dip) was used. By changing the local exposure dose by about a factor two, the local (positive) thermal expansion coefficient could be changed by about a factor of two. In this manner, 3D metamaterials composed of two different constituents were realized, allowing to flip the sign of the effective thermal expansion coefficient. In this complex 3D arrangement, the bending of bi-material beams was translated into a checkerboard arrangement of rotations and hence resulted in a structure shrinkage (Fig. 6a).

Along these lines, the Young's modulus, the Poisson's ratio, and viscoelasticity can also be controlled¹³⁵. Lemma et al. quantitatively analyzed commercial photoresists (Fig. 6b) including radical-initiated photo-cross-linked resists (IP series), a hybrid ceramic/polymer photosensitive resist (Ormocomp), and an epoxy-based resist (SU-8 2100). On this basis, cylindrical polymeric structures with

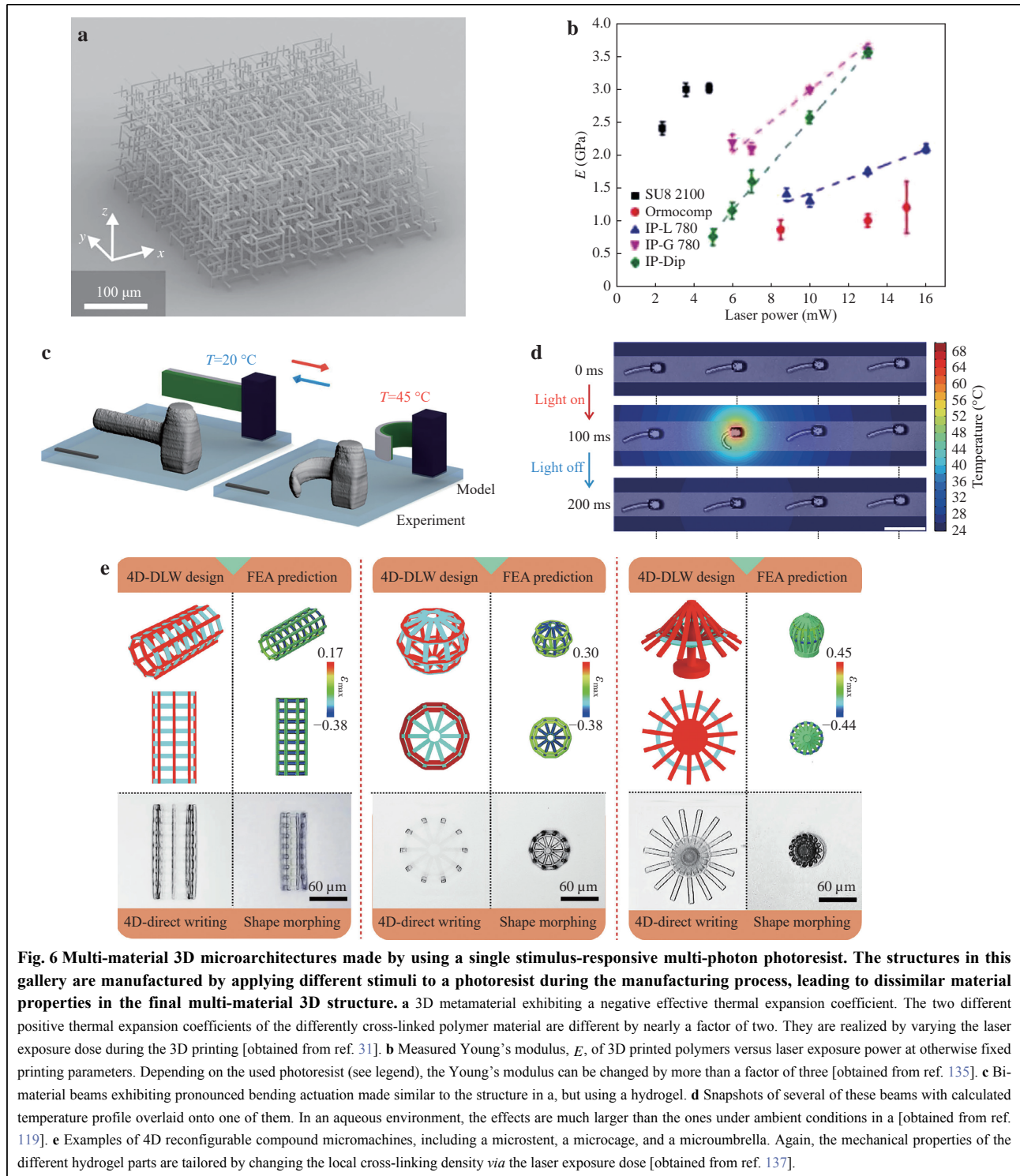
controlled Young's modulus and linear stiffness gradients were realized in a study of the invasion and migration of human colorectal adenocarcinoma (LS-174T) tumor cells with complex mechanical properties¹³⁶.

A closely related approach uses pNIPAM (see above)¹¹⁹. It should be noted though that this approach only works under aqueous conditions, whereas ref³¹ used ambient conditions. Differently designed responses were achieved using temperature and light as stimuli (Fig. 6c, d). Such approaches may find applications in 4D printing¹³⁷, microrobotics¹³⁸, and microsensors¹³⁹.

The local cross-linking density also determines the local polymer shrinkage during development and thereby the resulting local internal stress. In this manner, controllable residual stresses and programmable self-bending behavior of microstructures can be realized. Bauhofer et al. demonstrated the fabrication of bio-inspired objects with complex geometries and precisely controllable shape morphing¹⁴⁰.

Optical properties can also be modulated by controlling the cross-linking density of the photoresist. Dottermusch et al. systematically investigated the influence of the exposure dose on the refractive index of the commercial photoresist IP-Dip. A refractive-index difference of up to $\Delta n = 0.01$ was observed when changing the laser power from a minimum value to close to the explosion threshold¹⁴¹. The change in cross-linking density is also accompanied by a small volume change¹⁴².

Duan's group combined exposure-dose modulation with pH-responsive materials consisting of an acrylic acid (AAc) and N-isopropylacrylamide (NIPAM) as monomers, dipentaerythritol pentaacrylate (DPEPA) as cross-linker, 4,4'-bis (diethylamino) benzophenone (EMK) as photoinitiator, triethanolamine (TEA) as photosensitizer, and PVP as viscosity promoter¹³⁷. The final hydrogel structures exhibited excellent pH-responsive properties and were also sensitive to other stimuli, such as chemical solvents and temperature. By again controlling the local exposure dose, shape-morphing of the final structure was achieved. Rapid, precise, and reversible 3D-to-3D shape transformations for the construction of complex 3D reconfigurable compound micromachines were demonstrated (Fig. 6e). Similarly, Ling's group employed another kind of BSA-based pH-responsive material. By controlling the cross-linking density via the slicing distance at various regions with the same structure, the swelling extent of the microstructures can be quantified and controlled with high precision and anisotropic responsiveness across a single BSA structure can be achieved. For example, by patterning microstructures with



alternating low and high cross-linking section, reversible geometrical circle-to-polygon and polygon-to-circle shape morphing was achieved under pH changes²⁶. A free-standing 3D microtrap which is able to open and close in response to a pH change was also demonstrated²⁷.

Other examples include programming of the exposure dose by setting laser scanning path and scanning steps in solvent responsive photoresist, which enables reversible deformation and actuation of microstructures using different solvents¹³⁸, or by fabricating ion-responsive

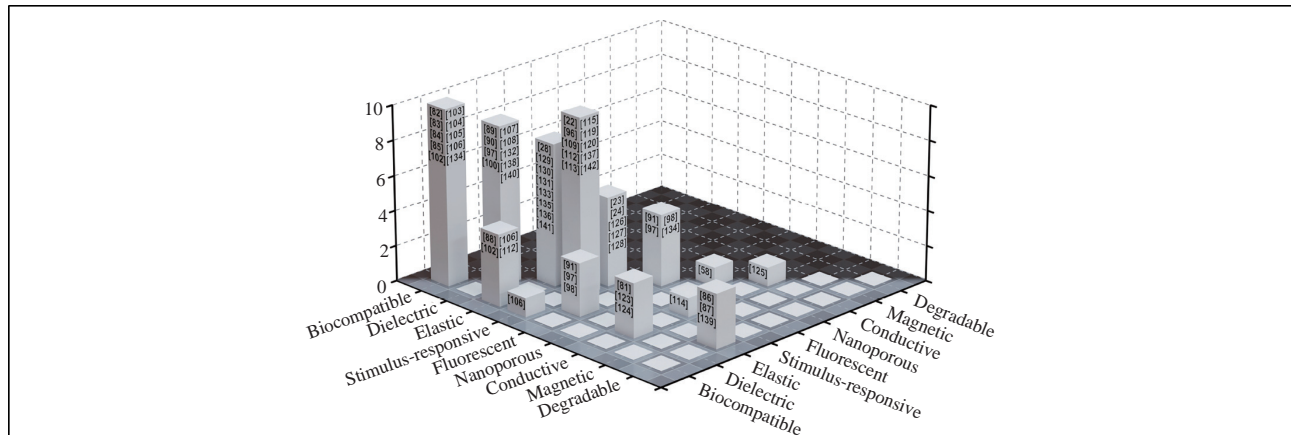


Fig. 7 Histogram of references reviewed in this paper addressing structures made by multi-photon 3D laser printing containing dissimilar ingredient material properties. For example, 9 papers reviewed here have presented multi-material architectures containing at least two different dielectric materials (entry dielectric-dielectric in this matrix). References may appear twice. For example, a stimulus-responsive material can at the same time be magnetic or elastic. The material properties are ordered according to the number of references occurring along the diagonal of this matrix. As the matrix is symmetric by definition, the redundant part is left away. The numbers in brackets on the side of the bars refer to the references summarized by the respective bar. Clearly, while some material-property combinations have been realized in several publications, several other material-property combinations have not so far.

microcantilevers using ionic responsive photoresist in a “bimaterial” based-design, leading to large bending angles of -33° within one second upon transferring the microcantilevers from water to sodium chloride solution¹³⁹.

The wavelength of the writing laser is another promising stimulus to modulate the material properties during 3D printing using a photoresist that is composed of two different subsystems susceptible to different wavelengths of light. In the ideal referred to as wavelength orthogonality, one wavelength leads to material property #1 and a second wavelength to material property #2. Even without such ideal orthogonality, the two wavelengths may result in significantly different properties. While several material systems have been reported based on one-photon polymerization process^{143–147}, this concept has so far not been demonstrated for multi-photon-based 3D laser printing. We briefly mention though that additive manufacturing by multi-photon polymerization at one wavelength and multi-photon subtractive manufacturing at another wavelength has been demonstrated¹⁴⁸.

Yet another stimulus is the writing laser optical polarization. For the SZ2080 organic–inorganic hybrid material, it has been shown that varying the polarization allows for controlling the polymerization process on a scale of nanometers, leading to the variations in width and symmetry of the 3D suspended polymerized bridges and photonic crystals under tight focusing¹⁴⁹. In a liquid-crystal-monomer photoresist, well controlled laser polarization facilitated the generation of tunable polymerization patterns¹⁵⁰. Furthermore, external topographical features can stimulate the alignment of the liquid-crystal director¹⁵¹.

Conclusions

We have reviewed the status of multi-material multi-photon 3D laser printing on the micrometer and nanometer scale. Fig. 7 provides a histogram of achieved combinations of dissimilar material properties reviewed here. Concerning primary materials, the field still shows shortcomings concerning electrically conductive, semiconducting, metallic, and stimuli-responsive ingredients. These can be combined to multi-material 3D architectures, e.g., by using an integrated microfluidic system. However, we have pointed out that such sequential 3D printing of dissimilar photoresists is prone to some fundamental restrictions connected to the fact that 3D laser printing fundamentally requires optically transparent photoresists or materials and that it requires small spatial modulations of the refractive index to avoid large optical aberrations during the printing process. Therefore, more recent approaches seek to use just a single (composite) photoresist and dedicated stimuli during the 3D printing process that allow defining the material properties locally within each voxel. However, these approaches are in their infancies and it is presently not clear yet what the fundamental limitations are.

Acknowledgements

The authors acknowledge funding by the Deutsche Forschungsgemeinschaft (DFG, German Research Foundation) under Germany’s Excellence Strategy for the Excellence Cluster “3D Matter Made to Order” (EXC 2082/1– 390761711), by the Carl Zeiss Foundation, by the Helmholtz program “Materials Systems Engineering (MSE)”, and by the Karlsruhe School of Optics and Photonics (KSOP).

Author details

¹Institute of Nanotechnology, Karlsruhe Institute of Technology (KIT), 76128 Karlsruhe, Germany. ²Institute of Applied Physics, Karlsruhe Institute of Technology (KIT), 76128 Karlsruhe, Germany. ³Institut für Organische Chemie, Ruprecht-Karls-Universität Heidelberg, Im Neuenheimer Feld 270, 69120 Heidelberg, Germany. ⁴Centre for Advanced Materials (CAM), Ruprecht-Karls-Universität Heidelberg, Im Neuenheimer Feld 225 and 270, 69120 Heidelberg, Germany

Author contributions

L. Yang: conceptualization, investigation, writing-original draft preparation, writing-review and editing.

F. Mayer: preparation of schematic figures, writing-review and editing.

U. Bunz: writing-review and editing, funding acquisition, project administration.

E. Blasco: conceptualization, investigation, writing-review and editing.

M. Wegener: conceptualization, writing-original draft preparation, writing-review and editing, funding acquisition, project administration, supervision.

Conflict of interest

The authors declare that they have no conflict of interest.

Received: 11 February 2021 Revised: 26 May 2021 Accepted: 26 May 2021

Accepted article preview online: 29 May 2021

Published online: 21 June 2021

References

- Ulichney, R. A. Void-and-cluster method for dither array generation. Proceedings of SPIE 1913, Human Vision, Visual Processing, and Digital Display IV. San Jose: SPIE, 1993.
- Swainson, W. K. DE1797599(A1), 1974.
- Hull, C. W. Patent history. (1986).
- Kodama, H. Automatic method for fabricating a three-dimensional plastic model with photo-hardening polymer. *Review of Scientific Instruments* **52**, 1770-1773 (1981).
- Maruo, S., Nakamura, O. & Kawata, S. Three-dimensional microfabrication with two-photon-absorbed photopolymerization. *Optics Letters* **22**, 132-134 (1997).
- Hahn, V. et al. Rapid assembly of small materials building blocks (Voxels) into large functional 3D metamaterials. *Advanced Functional Materials* **30**, 1907795 (2020).
- Hahn, V. et al. 3-D laser nanoprinting. *Optics and Photonics News* **30**, 28-35 (2019).
- Fischer, J. & Wegener, M. Three-dimensional optical laser lithography beyond the diffraction limit. *Laser & Photonics Reviews* **7**, 22-44 (2013).
- Gan, Z. S., Turner, M. D. & Gu, M. Biomimetic gyroid nanostructures exceeding their natural origins. *Science Advances* **2**, e1600084 (2016).
- Hentschel, M. et al. Chiral plasmonics. *Science Advances* **3**, e1602735 (2017).
- Thiel, M. et al. Dip-in depletion optical lithography of three-dimensional chiral polarizers. *Optics Letters* **38**, 4252-4255 (2013).
- Ergin, T., Fischer, J. & Wegener, M. Optical phase cloaking of 700 nm light waves in the far field by a three-dimensional carpet cloak. *Physical Review Letters* **107**, 173901 (2011).
- Kadic, M. et al. 3D metamaterials. *Nature Reviews Physics* **1**, 198-210 (2019).
- Ren, X. et al. Auxetic metamaterials and structures: a review. *Smart Materials and Structures* **27**, 023001 (2018).
- Surjadi, J. U. et al. Mechanical metamaterials and their engineering applications. *Advanced Engineering Materials* **21**, 1800864 (2019).
- Eder, M., Amini, S. & Fratzl, P. Biological composites—complex structures for functional diversity. *Science* **362**, 543-547 (2018).
- Kiefer, P. et al. Sensitive photoresists for rapid multiphoton 3D laser micro- and nanoprinting. *Advanced Optical Materials* **8**, 2000895 (2020).
- Sun, H. B. et al. Experimental investigation of single voxels for laser nanofabrication via two-photon photopolymerization. *Applied Physics Letters* **83**, 819-821 (2003).
- Mueller, J. B. et al. Polymerization kinetics in three-dimensional direct laser writing. *Advanced Materials* **26**, 6566-6571 (2014).
- Yang, L. et al. On the schwarzschild effect in 3D two-photon laser lithography. *Advanced Optical Materials* **7**, 1901040 (2019).
- Ma, Z. C. et al. Femtosecond-laser direct writing of metallic micro/nanostructures: from fabrication strategies to future applications. *Small Methods* **2**, 1700413 (2018).
- Saha, S. K. et al. Scalable submicrometer additive manufacturing. *Science* **366**, 105-109 (2019).
- Tudor, A. et al. Fabrication of soft, stimulus-responsive structures with sub-micron resolution via two-photon polymerization of poly(ionic liquids). *Materials Today* **21**, 807-816 (2018).
- Wei, S. X. et al. Protein-based 3D microstructures with controllable morphology and pH-responsive properties. *ACS Applied Materials & Interfaces* **9**, 42247-42257 (2017).
- Lv, C. et al. Humidity-responsive actuation of programmable hydrogel microstructures based on 3D printing. *Sensors and Actuators B: Chemical* **259**, 736-744 (2018).
- Lay, C. L. et al. Transformative two-dimensional array configurations by geometrical shape-shifting protein microstructures. *ACS Nano* **9**, 9708-9717 (2015).
- Lee, M. R. et al. Shape-shifting 3D Protein microstructures with programmable directionality via quantitative nanoscale stiffness modulation. *Small* **11**, 740-748 (2015).
- Marino, A. et al. Biomimicry at the nanoscale: current research and perspectives of two-photon polymerization. *Nanoscale* **7**, 2841-2850 (2015).
- Ovsianikov, A. et al. Engineering 3D cell-culture matrices: multiphoton processing technologies for biological and tissue engineering applications. *Expert Review of Medical Devices* **9**, 613-633 (2012).
- Soukoulis, C. M. & Wegener, M. Past achievements and future challenges in the development of three-dimensional photonic metamaterials. *Nature Photonics* **5**, 523-530 (2011).
- Qu, J. Y. et al. Micro-structured two-component 3D metamaterials with negative thermal-expansion coefficient from positive constituents. *Scientific Reports* **7**, 40643 (2017).
- Kern, C., Kadic, M. & Wegener, M. Experimental evidence for sign reversal of the hall coefficient in three-dimensional metamaterials. *Physical Review Letters* **118**, 016601 (2017).
- Frenzel, T., Kadic, M. & Wegener, M. Three-dimensional mechanical metamaterials with a twist. *Science* **358**, 1072-1074 (2017).
- Gissibl, T. et al. Two-photon direct laser writing of ultracompact multi-lens objectives. *Nature Photonics* **10**, 554-560 (2016).
- Schumann, M. F. et al. Cloaked contact grids on solar cells by coordinate transformations: designs and prototypes. *Optica* **2**, 850-853 (2015).
- Yang, L. et al. Parallel direct laser writing of micro-optical and photonic structures using spatial light modulator. *Optics and Lasers in Engineering* **70**, 26-32 (2015).
- Vizsnyiczai, G. et al. Light controlled 3D micromotors powered by bacteria. *Nature Communications* **8**, 15974 (2017).
- Huang, T. Y. et al. 3D printed microtransporters: compound

- micromachines for spatiotemporally controlled delivery of therapeutic agents. *Advanced Materials* **27**, 6644-6650 (2015).
39. Ceylan, H., Yasa, I. C. & Sitti, M. 3D chemical patterning of micromaterials for encoded functionality. *Advanced Materials* **29**, 1605072 (2017).
 40. Röhrig, M. et al. 3D direct laser writing of nano- and microstructured hierarchical gecko-mimicking surfaces. *Small* **8**, 3009-3015 (2012).
 41. Liu, X. J. et al. 3D printing of bioinspired liquid superrepellent structures. *Advanced Materials* **30**, 1800103 (2018).
 42. Dong, Z. Q. et al. Superoleophobic slippery lubricant-infused surfaces: combining two extremes in the same surface. *Advanced Materials* **30**, 1803890 (2018).
 43. Shi, Q. et al. Wiring up pre-characterized single-photon emitters by laser lithography. *Scientific Reports* **6**, 31135 (2016).
 44. Scordo, G. et al. A novel highly electrically conductive composite resin for stereolithography. *Materials Today Communications* **19**, 12-17 (2019).
 45. Greco, F. et al. Ultra-thin conductive free-standing PEDOT/PSS nanofilms. *Soft Matter* **7**, 10642-10650 (2011).
 46. Kurselis, K. et al. 3D fabrication of all-polymer conductive microstructures by two photon polymerization. *Optics Express* **21**, 31029-31035 (2013).
 47. Yamada, K., Yamada, Y. & Sone, J. Three-dimensional photochemical microfabrication of poly(3, 4-ethylene-dioxythiophene) in transparent polymer sheet. *Thin Solid Films* **554**, 102-105 (2014).
 48. Skotheim, T.A. & Reynolds, J. R. *Handbook of Conducting Polymers*. (London: CRC Press, 2007).
 49. Chandrasekhar, P. *Conducting Polymers, Fundamentals and Applications: A Practical Approach*. (Boston: Springer, 1999).
 50. Agarwal, N. et al. Direct writing of a conducting polymer pattern in aqueous solution by using an ultrashort laser pulse. *RSC Advances* **7**, 38565-38569 (2017).
 51. Ishikawa, A., Tanaka, T. & Kawata, S. Improvement in the reduction of silver ions in aqueous solution using two-photon sensitive dye. *Applied Physics Letters* **89**, 113102 (2006).
 52. Cao, Y. Y. et al. 3D metallic nanostructure fabrication by surfactant-assisted multiphoton-induced reduction. *Small* **5**, 1144-1148 (2009).
 53. Blasco, E. et al. Fabrication of conductive 3D gold-containing microstructures via direct laser writing. *Advanced Materials* **28**, 3592-3595 (2016).
 54. Shukla, S. et al. Two-photon lithography of sub-wavelength metallic structures in a polymer matrix. *Advanced Materials* **22**, 3695-3699 (2010).
 55. Zarzar, L. D. et al. Multiphoton lithography of nanocrystalline platinum and palladium for site-specific catalysis in 3D microenvironments. *Journal of the American Chemical Society* **134**, 4007-4010 (2012).
 56. Ma, Z. C. et al. Femtosecond laser direct writing of plasmonic Ag/Pd alloy nanostructures enables flexible integration of robust SERS substrates. *Advanced Materials Technologies* **2**, 1600270 (2017).
 57. Lee, M. R. et al. Direct metal writing and precise positioning of gold nanoparticles within microfluidic channels for SERS sensing of gaseous analytes. *ACS Applied Materials & Interfaces* **9**, 39584-39593 (2017).
 58. Xu, B. B. et al. Flexible nanowiring of metal on nonplanar substrates by femtosecond-laser-induced electroless plating. *Small* **6**, 1762-1766 (2010).
 59. Tabrizi, S. et al. Functional optical plasmonic resonators fabricated via highly photosensitive direct laser reduction. *Advanced Optical Materials* **4**, 529-533 (2016).
 60. Mayer, F. et al. 3D two-photon microprinting of nanoporous architectures. *Advanced Materials* **32**, 2002044 (2020).
 61. Lindenmann, N. et al. Connecting silicon photonic circuits to multicore fibers by photonic wire bonding. *Journal of Lightwave Technology* **33**, 755-760 (2015).
 62. Wong, S. et al. Direct laser writing of three-dimensional photonic crystals with a complete photonic bandgap in chalcogenide glasses. *Advanced Materials* **18**, 265-269 (2006).
 63. Cumming, B. P. et al. Adaptive aberration compensation for three-dimensional micro-fabrication of photonic crystals in lithium niobate. *Optics Express* **19**, 9419-9425 (2011).
 64. Ródenas, A. et al. Rare-earth spontaneous emission control in three-dimensional lithium niobate photonic crystals. *Advanced Materials* **21**, 3526-3530 (2009).
 65. Ovsianikov, A. et al. Ultra-low shrinkage hybrid photosensitive material for two-photon polymerization microfabrication. *ACS Nano* **2**, 2257-2262 (2008).
 66. Sakellari, I. et al. Two-photon polymerization of titanium-containing sol-gel composites for three-dimensional structure fabrication. *Applied Physics A* **100**, 359-364 (2010).
 67. Kotz, F. et al. Two-photon polymerization of nanocomposites for the fabrication of transparent fused silica glass microstructures. *Advanced Materials* **33**, 2006341 (2021).
 68. Doualle, T., André, J. C. & Gallais, L. 3D printing of silica glass through a multiphoton polymerization process. *Optics Letters* **46**, 364-367 (2021).
 69. Arita, R. et al. Rapid three-dimensional structuring of transparent SiO₂ glass using interparticle photo-cross-linkable suspensions. *Communications Materials* **1**, 30 (2020).
 70. Ródenas, A. et al. Three-dimensional femtosecond laser nanolithography of crystals. *Nature Photonics* **13**, 105-109 (2019).
 71. Cooperstein, I. et al. 3D printing of micrometer-sized transparent ceramics with on-demand optical-gain properties. *Advanced Materials* **32**, 2001675 (2020).
 72. Hippler, M. et al. 3D scaffolds to study basic cell biology. *Advanced Materials* **31**, 1808110 (2019).
 73. Zhou, W. H. et al. An efficient two-photon-generated photoacid applied to positive-tone 3D microfabrication. *Science* **296**, 1106-1109 (2002).
 74. Connell, J. L. et al. 3D printing of microscopic bacterial communities. *Proceedings of the National Academy of Sciences of the United States of America* **110**, 18380-18385 (2013).
 75. Ovsianikov, A. et al. Laser fabrication of 3D gelatin scaffolds for the generation of bioartificial tissues. *Materials* **4**, 288-299 (2011).
 76. Kufelt, O. et al. Water-soluble photopolymerizable chitosan hydrogels for biofabrication via two-photon polymerization. *Acta Biomaterialia* **18**, 186-195 (2015).
 77. Kaehr, B. & Shear, J. B. Multiphoton fabrication of chemically responsive protein hydrogels for microactuation. *Proceedings of the National Academy of Sciences of the United States of America* **105**, 8850-8854 (2008).
 78. Basu, S. & Campagnola, P. J. Properties of crosslinked protein matrices for tissue engineering applications synthesized by multiphoton excitation. *Journal of Biomedical Materials Research Part A* **71A**, 359-368 (2004).
 79. Spiegel, C. A. et al. 4D printing at the microscale. *Advanced Functional Materials* **30**, 1907615 (2020).
 80. Xiong, W. et al. Laser-directed assembly of aligned carbon nanotubes in three dimensions for multifunctional device fabrication. *Advanced Materials* **28**, 2002-2009 (2016).
 81. Masui, K. et al. Laser fabrication of Au nanorod aggregates microstructures assisted by two-photon polymerization. *Optics Express* **19**, 22786-22796 (2011).
 82. Peters, C. et al. Degradable magnetic composites for minimally

- invasive interventions: device fabrication, targeted drug delivery, and cytotoxicity tests. *Advanced Materials* **28**, 533-538 (2016).
83. Xin, C. et al. Conical hollow microhelices with superior swimming capabilities for targeted cargo delivery. *Advanced Materials* **31**, 1808226 (2019).
 84. Yang, L. et al. Targeted single-cell therapeutics with magnetic tubular micromotor by one-step exposure of structured femtosecond optical vortices. *Advanced Functional Materials* **29**, 1905745 (2019).
 85. Marino, A. et al. Two-photon lithography of 3D nanocomposite piezoelectric scaffolds for cell stimulation. *ACS Applied Materials & Interfaces* **7**, 25574-25579 (2015).
 86. Saha, S. K. et al. Kinematic fixtures to enable multi-material printing and rapid non-destructive inspection during two-photon lithography. *Precision Engineering* **54**, 131-137 (2018).
 87. Waller, E. H., Renner, M. & von Freymann, G. Active aberration- and point-spread-function control in direct laser writing. *Optics Express* **20**, 24949-24956 (2012).
 88. Takeyasu, N., Tanaka, T. & Kawata, S. Fabrication of 3D metal/polymer microstructures by site-selective metal coating. *Applied Physics A* **90**, 205-209 (2008).
 89. Klein, F. et al. Two-component polymer scaffolds for controlled three-dimensional cell culture. *Advanced Materials* **23**, 1341-1345 (2011).
 90. Da Sie, Y. et al. Fabrication of three-dimensional multi-protein microstructures for cell migration and adhesion enhancement. *Biomedical Optics Express* **6**, 480-490 (2015).
 91. Claus, T. K. et al. Simultaneous dual encoding of three-dimensional structures by light-induced modular ligation. *Angewandte Chemie International Edition* **55**, 3817-3822 (2016).
 92. Richter, B. et al. Guiding cell attachment in 3D microscaffolds selectively functionalized with two distinct adhesion proteins. *Advanced Materials* **29**, 1604342 (2017).
 93. Zieger, M. M. et al. Cleaving direct-laser-written microstructures on demand. *Angewandte Chemie International Edition* **56**, 5625-5629 (2017).
 94. Zieger, M. M. et al. A subtractive photoresist platform for micro- and macroscopic 3D printed structures. *Advanced Functional Materials* **28**, 1801405 (2018).
 95. Gernhardt, M. et al. Multi-material 3D microstructures with photochemically adaptive mechanical properties. *Journal of Materials Chemistry C* **8**, 10993-11000 (2020).
 96. Malinauskas, M. et al. 3D microporous scaffolds manufactured via combination of fused filament fabrication and direct laser writing ablation. *Micromachines* **5**, 839-858 (2014).
 97. Malinauskas, M. et al. Ultrafast laser processing of materials: from science to industry. *Light: Science & Applications* **5**, e16133 (2016).
 98. Mayer, F. et al. 3D fluorescence-based security features by 3D laser lithography. *Advanced Materials Technologies* **2**, 1700212 (2017).
 99. Maruyama, T. et al. Multi-material microstereolithography using a palette with multicolor photocurable resins. *Optical Materials Express* **10**, 2522-2532 (2020).
 100. Choi, J. W., Kim, H. C. & Wicker, R. Multi-material stereolithography. *Journal of Materials Processing Technology* **211**, 318-328 (2011).
 101. Wang, Q. M. et al. Lightweight mechanical metamaterials with tunable negative thermal expansion. *Physical Review Letters* **117**, 175901 (2016).
 102. Kowsari, K. et al. High-efficiency high-resolution multimaterial fabrication for digital light processing-based three-dimensional printing. *3D Printing and Additive Manufacturing* **5**, 185-193 (2018).
 103. Ma, Z. C. et al. Femtosecond laser programmed artificial musculoskeletal systems. *Nature Communications* **11**, 4536 (2020).
 104. Lamont, A. C. et al. A facile multi-material direct laser writing strategy. *Lab on a Chip* **19**, 2340-2345 (2019).
 105. Mayer, F. et al. Multimaterial 3D laser microprinting using an integrated microfluidic system. *Science Advances* **5**, eaau9160 (2019).
 106. Pregibon, D. C., Toner, M. & Doyle, P. S. Multifunctional encoded particles for high-throughput biomolecule analysis. *Science* **315**, 1393-1396 (2007).
 107. Laza, S. C. et al. Two-photon continuous flow lithography. *Advanced Materials* **24**, 1304-1308 (2012).
 108. Richter, B. et al. Three-dimensional microscaffolds exhibiting spatially resolved surface chemistry. *Advanced Materials* **25**, 6117-6122 (2013).
 109. Brand, C. A. et al. Tension and elasticity contribute to fibroblast cell shape in three dimensions. *Biophysical Journal* **113**, 770-774 (2017).
 110. Scheiwe, A. C. et al. Subcellular stretch-induced cytoskeletal response of single fibroblasts within 3D designer scaffolds. *Biomaterials* **44**, 186-194 (2015).
 111. Serien, D. & Takeuchi, S. Multi-component microscaffold with 3D spatially defined proteinaceous environment. *ACS Biomaterials Science & Engineering* **3**, 487-494 (2017).
 112. Wollhofen, R. et al. Multiphoton-polymerized 3D protein assay. *ACS Applied Materials & Interfaces* **10**, 1474-1479 (2018).
 113. Hippler, M. et al. Mechanical stimulation of single cells by reversible host-guest interactions in 3D microscaffolds. *Science Advances* **6**, eabc2648 (2020).
 114. Schmid, M. et al. Three-dimensional direct laser written achromatic axicons and multi-component microlenses. *Optics Letters* **43**, 5837-5840 (2018).
 115. Gissibl, T. et al. Sub-micrometre accurate free-form optics by three-dimensional printing on single-mode fibres. *Nature Communications* **7**, 11763 (2016).
 116. Nocentini, S. et al. Three-dimensional photonic circuits in rigid and soft polymers tunable by light. *ACS Photonics* **5**, 3222-3230 (2018).
 117. Nocentini, S. et al. 3D printed photoresponsive materials for photonics. *Advanced Optical Materials* **7**, 1900156 (2019).
 118. Zhu, W. et al. 3D-printed artificial microfish. *Advanced Materials* **27**, 4411-4417 (2015).
 119. Hippler, M. et al. Controlling the shape of 3D microstructures by temperature and light. *Nature Communications* **10**, 232 (2019).
 120. Nishiguchi, A. et al. In-gel direct laser writing for 3D-designed hydrogel composites that undergo complex self-shaping. *Advanced Science* **5**, 1700038 (2018).
 121. Nishiyama, H., Odashima, S. & Asoh, S. Femtosecond laser writing of plasmonic nanoparticles inside PNIPAM microgels for light-driven 3D soft actuators. *Optics Express* **28**, 26470-26480 (2020).
 122. Xiong, Z. et al. Fast solvent-driven micropump fabricated by two-photon microfabrication. *Applied Physics A* **93**, 447-452 (2008).
 123. Tian, Y. et al. Solvent response of polymers for micromachine manipulation. *Physical Chemistry Chemical Physics* **13**, 4835-4838 (2011).
 124. Ohm, C., Brehmer, M. & Zentel, R. Liquid crystalline elastomers as actuators and sensors. *Advanced Materials* **22**, 3366-3387 (2010).
 125. Xie, P. & Zhang, R. B. Liquid crystal elastomers, networks and gels: advanced smart materials. *Journal of Materials Chemistry* **15**, 2529-2550 (2005).
 126. Zeng, H. et al. Light robots: bridging the gap between microrobotics and photomechanics in soft materials. *Advanced Materials* **30**, 1703554 (2018).
 127. Nocentini, S. et al. Optically driven soft micro robotics. *Advanced Optical Materials* **6**, 1800207 (2018).
 128. Zeng, H. et al. Light-fueled microscopic walkers. *Advanced Materials* **27**, 3883-3887 (2015).
 129. Martella, D. et al. Photonic microhand with autonomous action. *Advanced Materials* **29**, 1704047 (2017).

130. Tanaka, T., Ishikawa, A. & Kawata, S. Two-photon-induced reduction of metal ions for fabricating three-dimensional electrically conductive metallic microstructure. *Applied Physics Letters* **88**, 081107 (2006).
131. Kang, S., Vora, K. & Mazur, E. One-step direct-laser metal writing of sub-100 nm 3D silver nanostructures in a gelatin matrix. *Nanotechnology* **26**, 121001 (2015).
132. Farrer, R. A. et al. Selective functionalization of 3-D polymer microstructures. *Journal of the American Chemical Society* **128**, 1796-1797 (2006).
133. LaFratta, C. N. et al. Direct laser patterning of conductive wires on three-dimensional polymeric microstructures. *Chemistry of Materials* **18**, 2038-2042 (2006).
134. Machida, M. et al. Spatially-targeted laser fabrication of multi-metal microstructures inside a hydrogel. *Optics Express* **27**, 14657-14666 (2019).
135. Lemma, E. D. et al. Mechanical properties tunability of three-dimensional polymeric structures in two-photon lithography. *IEEE Transactions on Nanotechnology* **16**, 23-31 (2017).
136. Lemma, E. D. et al. Tunable mechanical properties of stent-like microscaffolds for studying cancer cell recognition of stiffness gradients. *Microelectronic Engineering* **190**, 11-18 (2018).
137. Jin, D. D. et al. Four-dimensional direct laser writing of reconfigurable compound micromachines. *Materials Today* **32**, 19-25 (2020).
138. Zhang, Y. L. et al. Dual-3D femtosecond laser nanofabrication enables dynamic actuation. *ACS Nano* **13**, 4041-4048 (2019).
139. Xiong, Z. et al. Asymmetric microstructure of hydrogel: two-photon microfabrication and stimuli-responsive behavior. *Soft Matter* **7**, 10353-10359 (2011).
140. Bauhofer, A. A. et al. Harnessing photochemical shrinkage in direct laser writing for shape morphing of polymer sheets. *Advanced Materials* **29**, 1703024 (2017).
141. Dottermusch, S. et al. Exposure-dependent refractive index of Nanoscribe IP-Dip photoresist layers. *Optics Letters* **44**, 29-32 (2019).
142. de Miguel, G. et al. $\lambda/20$ axial control in 2.5D polymerized structures fabricated with DLW lithography. *Optics Express* **23**, 24850-24858 (2015).
143. Batchelor, R. R. et al. Spatially resolved coding of λ -orthogonal hydrogels by laser lithography. *Chemical Communications* **54**, 2436-2439 (2018).
144. Dolinski, N. D. et al. Solution Mask Liquid Lithography (SMaLL) for one-step, multimaterial 3D printing. *Advanced Materials* **30**, 1800364 (2018).
145. Bialas, S. et al. Access to disparate soft matter materials by curing with two colors of light. *Advanced Materials* **31**, 1807288 (2019).
146. Schwartz, J. J. & Boydston, A. J. Multimaterial actinic spatial control 3D and 4D printing. *Nature Communications* **10**, 791 (2019).
147. Kaupp, M. et al. Wavelength selective polymer network formation of end-functional star polymers. *Chemical Communications* **52**, 1975-1978 (2016).
148. Batchelor, R. et al. Two in one: light as a tool for 3d printing and erasing at the microscale. *Advanced Materials* **31**, 1904085 (2019).
149. Reškštytė, S. et al. Nanoscale precision of 3D Polymerization via polarization control. *Advanced Optical Materials* **4**, 1209-1214 (2016).
150. Jisha, C. P. et al. Tunable pattern transitions in a liquid-crystal-monomer mixture using two-photon polymerization. *Optics Letters* **37**, 4931-4933 (2012).
151. Guo, Y. B., Shahsavan, H. & Sitti, M. 3D microstructures of liquid crystal networks with programmed voxelated director fields. *Advanced Materials* **32**, 2002753 (2020).